Chaos, Solitons and Fractals 171 (2023) 113453

Contents lists available at ScienceDirect

Chaos, Solitons and Fractals

journal homepage: www.elsevier.com/locate/chaos

Spatial permutation entropy distinguishes resting brain states

Bruno R.R. Boaretto [a,*], Roberto C. Budzinski [b,c,d], Kalel L. Rossi [e], Cristina Masoller [f,*], Elbert E.N. Macau [a]

[a] Institute of Science and Technology, Federal University of Sao Paulo, Sao Jose dos Campos, Sao Paulo, Brazil
[b] Department of Mathematics, Western University, London, Ontario, Canada
[c] Western Institute for Neuroscience, Western University, London, Ontario, Canada
[d] Western Academy for Advanced Research, Western University, London, Ontario, Canada
[e] Theoretical Physics Complex Systems, Carl von Ossietzky University Oldenburg, Oldenburg, Lower Saxony, Germany
[f] Department of Physics, Universitat Politecnica de Catalunya, Terrassa, Barcelona, Spain

ARTICLE INFO

Keywords:
Time series analysis
Ordinal analysis
EEG

ABSTRACT

We use ordinal analysis and spatial permutation entropy to distinguish between eyes-open and eyes-closed resting brain states. To do so, we analyze EEG data recorded with 64 electrodes from 109 healthy subjects, under two one-minute baseline runs: One with eyes open, and one with eyes closed. We use spatial ordinal analysis to distinguish between these states, where the permutation entropy is evaluated considering the spatial distribution of electrodes for each time instant. We analyze both raw and post-processed data considering only the alpha-band frequency (8–12 Hz) which is known to be important for resting states in the brain. We conclude that spatial ordinal analysis captures information about correlations between time series in different electrodes. This allows the discrimination of eyes closed and eyes open resting states in both raw and filtered data. Filtering the data only amplifies the distinction between states. Importantly, our approach does not require EEG signal pre-processing, which is an advantage for real-time applications, such as brain-computer interfaces.

1. Introduction

Ordinal analysis, proposed by Bandt and Pompe [1], has been used for over 20 years to extract useful information about the underlying system from data [2,3]. In particular, the so-called permutation entropy encodes the information about the probability distributions of ordinal patterns of a given time series. Ordinal patterns are used to describe the intricate dynamical patterns of a system and can be used in several ways: as a complexity measure [4,5], to identify characteristic time scales [6–8], to distinguish between stochastic and deterministic systems [4,9–11], to detect synchronization at different time scales [12], etc. Ordinal analysis has found applications in a diversity of scientific fields including biomedicine [13–16], economy [17], optics [18], climatology [19–21], and neuroscience [22–25] among many others.

Here we use the ordinal method to analyze electroencephalography (EEG) brain signals. EEG is routinely used in clinical studies to detect and investigate abnormal brain activity and its noninvasive nature is a key advantage for brain-computer interface (BCI) technologies [26]. EEG is typically described in terms of rhythmic activity in frequency bands: δ-band $\in$ $(0, 4)$ Hz, θ-band $\in$ $[4, 8)$ Hz, α-band $\in$ $[8, 12)$ Hz, β-band $\in$ $[12, 30)$ Hz, γ-band $\in$ $[30, \infty)$ Hz. These bands are associated with a dominant frequency regime of significant biological importance [27,28]. In particular, the α-band observed in EEG over the human posterior cortex is prominent in normal individuals during eyes-closed (EC) resting and attenuates during eyes-open (EO) resting [29,30]. Several methods have been proposed to detect EC to EO states, e.g. the Fourier transform to estimate the difference between the mean α-band components [30,31]; second-order difference plot and signal processing techniques to investigate differences in the EEG time series [32]; statistical feature analysis in association with artificial intelligence classifiers [33–36].

The EC–EO transition has also been studied using ordinal analysis. Quintero-Queiros et al. [22] have analyzed the permutation entropy, the transition entropy, and the asymmetry coefficient of two EEG datasets with different spatial and temporal resolutions examining both raw data and post-processed data. They found that, on average, the eyes open state is characterized by higher entropy values, although, due to the large variability of the standard deviation, the permutation entropy does not allow full discrimination between the two states.

* Corresponding authors.
E-mail addresses: brrb12@fisica.ufpr.br (B.R.R. Boaretto), rbudzins@uwo.ca (R.C. Budzinski), kalel.rossi@uni-oldenburg.de (K.L. Rossi), cristina.masoller@upc.edu (C. Masoller), elbert.macau@unifesp.br (E.E.N. Macau).

https://doi.org/10.1016/j.chaos.2023.113453
Received 14 March 2023; Accepted 11 April 2023
Available online 28 April 2023

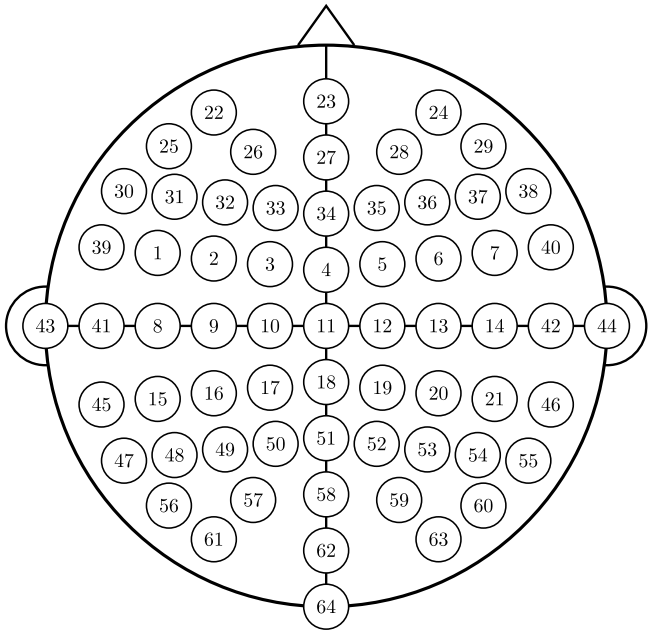

Fig. 1. Spatial arrangement of the 64 electrodes. Here we show a schematic representation of the electrodes during the recording of the data [43].

Recently, several studies in neuroscience have shown the importance of analyzing the spatial and temporal behavior of a given system. By considering the spatial aspect of the neural system, complex patterns can be observed in different scales [37,38]. These patterns are thought to play important roles in brain functioning [38,39]. In this paper, we discriminate between EO and EC states using ordinal analysis and spatial permutation entropy [40–42]. Assuming that correlations between signals recorded in different electrodes encode valuable spatial information, we evaluate the spatial permutation entropy (spatial PE). We show that the spatial PE allows full discrimination between states and, as expected, the discrimination is more pronounced in the filtered data. To show that the spatial information is relevant to the results, the information from electrodes is shuffled so that the spatial relation in the data is annihilated, our approach no longer allows the distinction between states. Finally, we successfully apply our method to short time series of EEG data, which indicates that our method may be extended for "online" analyses.

This paper is organized as follows: Section 2 presents the dataset and details of the methodology used in this work, Section 3 presents the results, and Section 4 presents the discussion and our conclusions.

2. Data and methods

2.1. Dataset

We use a freely available dataset [43–45] composed of EEG data from 109 healthy subjects. Each subject performed two one-minute baseline runs with an eyes-closed state (EC) and eyes-opened state (EO). The EEG was recorded from 64 electrodes that are spatially arranged as shown in Fig. 1. Table 1 presents the description of the dataset. More information about the experimental setup and subjects can be found in Ref. [43]. We have discarded subjects #97 and #109 due to several null values at the end of the time series.

In this work, we study both the raw time series and the filtered time series in which only the components of the α-band are selected. To filter the data, we have used a bandpass *Butterworth* filter using the *Scipy* open library [46] applied to the whole time-series. Fig. 2 depicts a typical EEG signal from subject #1 during the EC state (upper panels) and EO state (bottom panels). Panel (a) depicts the raw signal of the EC state and panel (b) is the filtered signal. Panel (d) shows the raw signal of the EO state and panel (e) is the filtered signal. By comparing the upper and bottom rows, we notice that it is hard to distinguish the EC and EO states with the naked eye (either in the raw data or filtered data). Panels (c) and (f) present the magnification of the gray area of the filtered data (from 1 to 4 s). These panels illustrate that differences can be spotted in EEG time series when these are displayed in a short time scale.

Table 1
Description of the dataset.

Sampling rate	160 Hz
Time per task	60 s
Total points per task	9600
Number of electrodes	64
Number of subjects	109

2.2. Ordinal analysis and permutation entropy

Ordinal analysis and permutation entropy allow the identification of nonlinear patterns and relations in complex time series [1]. In a time series of τ points, each sequence of D points can be associated with an ordinal pattern, where the D values are replaced by their relative amplitudes, ordered from 0 to $D-1$. Therefore, $D!$ is the number of possible patterns, which for $D=3$, illustrated in Fig. 3, is 6. For example, the sequence of three data points $x=\{1.1, 1.2, 3.8\}$ becomes pattern $s(x)=\{0, 1, 2\}$, while $x=\{32, -0.52, 4.7\}$ becomes $s(x)=\{2, 0, 1\}$.

For a time series of τ points, we have $\tau-(D-1)$ sequences of D points to be analyzed. For each pattern i, its ordinal probability $P(i)$ is then computed as its frequency of occurrence with $\sum_{i=1}^{D!} P(i)=1$, where i represents each pattern. Then, the permutation entropy [1] is evaluated as:

$$S=-\sum_{i=1}^{D!} P(i)\log P(i). \tag{1}$$

The permutation entropy varies from $S=0$ if the j^{th} state $P(j)=1$ while $P(i)=0\ \forall\ i\neq j$ to $S=\log D!$ if $P(i)=1/D!\ \forall\ i$. The normalized permutation entropy is given by:

$$H=\frac{S(D)}{\log D!}. \tag{2}$$

As explained in the introduction, we assume that relations between signals recorded in different electrodes, positioned in different locations on the scalp, encode valuable spatial information. Therefore, we evaluate the spatial permutation entropy (spatial PE) using the approach illustrated in Fig. 4. Particularly, we evaluate the permutation entropy of the electrodes for each time instant for each subject, considering exactly the disposition of the data in the form in which they were published [43]. Being H_i^t the spatial PE of the i^{th} subject at time t^{th}, this results in $\tau=9600$ values of spatial PE per subject that are used to characterize the EC and EO states. The average over all subjects at time t is

$$\bar{H}^t=\frac{1}{N}\sum_{i=1}^{N} H_i^t, \tag{3}$$

and the mean entropy $\langle\bar{H}\rangle$ is the average over time

$$\langle\bar{H}\rangle=\frac{1}{\tau}\sum_{t=1}^{\tau}\bar{H}^t. \tag{4}$$

$\langle\bar{H}\rangle$ and the standard deviation

$$\sigma=\sqrt{\frac{\sum_{t=1}^{\tau}(\bar{H}^t-\langle\bar{H}\rangle)^2}{\tau-1}}, \tag{5}$$

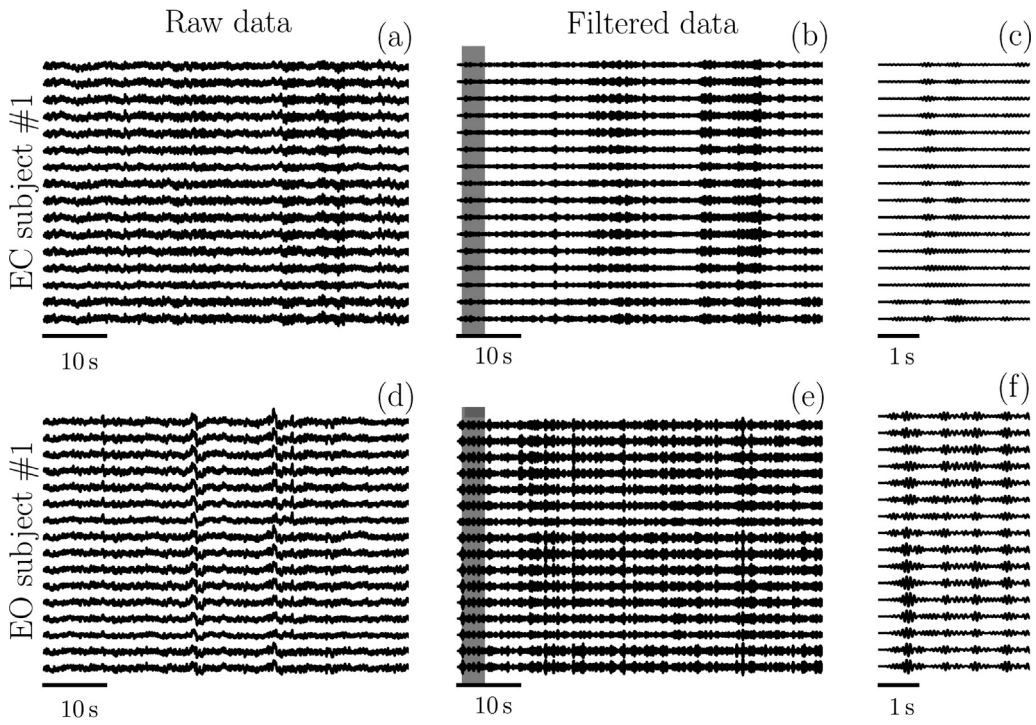

Fig. 2. Examples of EEG signals analyzed in this work. Representation of the first 16 electrodes of subject #1 during EC state (upper) and EO state (bottom): **(a)**, and **(d)** raw data; **(b)** and **(e)** filtered data. Panels **(c)** and **(f)** depict the magnification of the gray rectangles $[1-4]$ s of the filtered data.

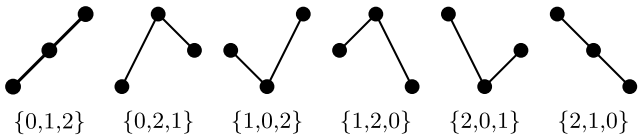

Fig. 3. Representation of the ordinal patterns. Schematic illustration of the 6 ordinal patterns that can be defined from $D = 3$ consecutive data values in a given time series.

are used to distinguish EC and EO states.

The dataset is composed of 64 electrodes, which limits the size of the ordinal pattern, D, that we can use. If D is too large, we do not have enough patterns to accurately estimate ordinal probabilities, while if D is too small, we do not capture spatial relationships. As a compromise, we selected $D = 3$, which allows us to obtain, for each subject at a given time t, 62 ordinal patterns. We use them to estimate, at time t, the probabilities of the 6 ordinal patterns of length $D = 3$ (illustrated in Fig. 3). A robust estimation of the probabilities requires that the number of available patterns is at least 10 times the number of possible patterns, and we show here that a good distinction of the EC and EO states can be obtained with 62 $D = 3$ ordinal patterns.

3. Results

Fig. 5(a) shows the average of the spatial permutation entropy $\bar{H}^t$ over all subjects for each time instant. Panel (b) depicts the mean values over all time instants for each state $\langle \bar{H} \rangle$, the error bars represent one standard deviation from the mean value (Eq. (5)). We observe that the EO state has a higher mean value than the EC state, which is consistent with the results shown in Ref. [22]; however, in our results, there is no overlap between the error bars. Therefore by using the methodology presented in our work, the two states can be distinguished at least over one standard deviation. Figs. 5 (c) and (d) depict the same analysis for the filtered data, where we can notice, as expected, that distinction between the states is more pronounced.

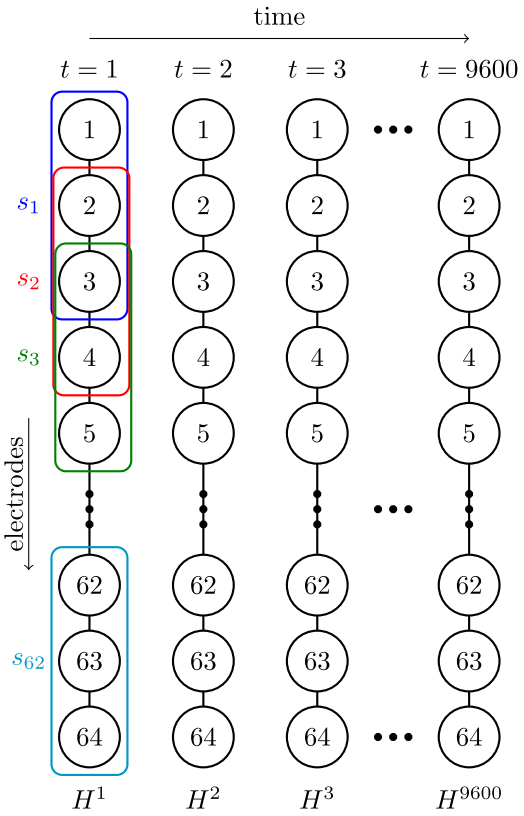

Fig. 4. Spatial ordinal analysis. The ordinal patterns are extracted from data at each time instant according to the spatial distribution of the electrodes (Fig. 1). At each time step t the first pattern s_1 is computed from electrodes $\{1, 2, 3\}$, the second s_2, from $\{2, 3, 4\}$, the third s_3, from $\{3, 4, 5\}$, and so on until the last pattern s_{62} is computed from electrodes $\{62, 63, 64\}$. With these patterns $(s_1 \ldots s_{64})$ the ordinal probabilities, P_i with $i = 1 \ldots 6$, are calculated, and then the value of the spatial permutation entropy at time t is calculated using Eq. (2).

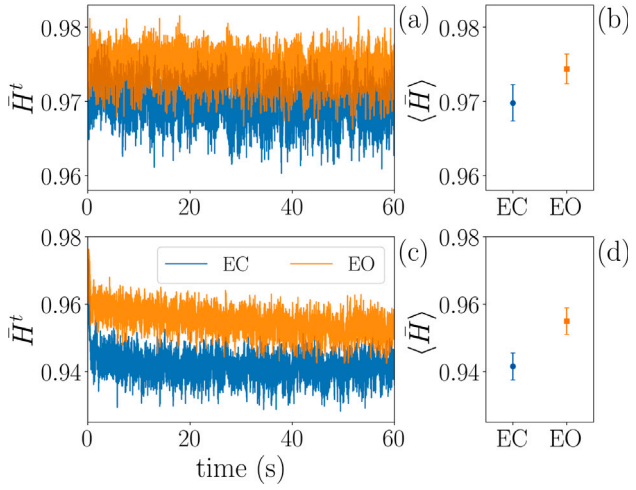

Fig. 5. Spatial ordinal analysis distinguishes EC and EO states. **((a), (c))** Average over subjects of each state $\bar{H}^t$ for each time instant (Eq. (3)); **((b), (d))** Mean values over all time instants $\langle \bar{H} \rangle$ (Eq. (4)). The error bars display one standard deviation over the mean value (Eq. (5)) of each state. The upper panels present the results of the raw data and the bottom panels the filtered data.

All the spatial ordinal analysis is done by assuming that the electrodes encode spatial information, and the ordinal patterns are extracted following exactly the arrangement available in the dataset that coincides with the indices of the electrodes (Fig. 1). Fig. 6 presents the same spatial analysis of Fig. 5 but we made a preliminary exploration of a different spatial configuration of the electrodes (panel (a)). Figs. 6 (b–e) present the spatial PE $\langle \bar{H} \rangle$ of each state, illustrating that another spatial arrangement of the electrodes slightly enhances the separation between states, i.e., improving the performance of spatial ordinal analysis in distinguishing between the EC and EO states.

The spatial information encoded in the electrodes can be destroyed if we shuffled the electrodes, i.e., randomly permute the electrode in space. This procedure is analogous to that performed in temporal ordinal analysis, where any short and long-distance temporal correlation information is lost when a time series is shuffled. The results obtained from the shuffled electrodes are depicted in Fig. 7 following the same methodology of Fig. 5. We observe an increase in mean entropy $\langle \bar{H} \rangle$ of the states for both raw and filtered data, which is expected due to the loss of the spatial correlation. Figs. 7(b,d) show that when the spatial information is washed out by the shuffling, the distinction between EO and EC states is not possible. The positions of the electrodes are shuffled in the same way for all the subjects.

In ordinal analysis, the probabilities of the ordinal patterns may carry valuable information [2]. As we have shown, the spatial permutation entropy is able to distinguish between the resting brain states. With this in mind, we can take a step back and analyze how the ordinal probabilities differ in states EC and EO. As explained before, at each time, 62 patterns of length 3 are obtained (from the values in the 64 electrodes at that time) and the 6 probabilities are computed. By averaging over time, we obtain, for each probability, a mean value and a standard deviation, which are shown in Fig. 8. Here, circles represent the EC state, squares the EO state, and bars represent the standard deviation. The 6 rows show the 6 ordinal probabilities and the left (right) column presents the results of the raw (filtered) data. In this figure, we observe that some patterns are more informative for distinguishing the EO and EC states. Specifically, in the raw data, pattern $\{0, 2, 1\}$ allows a good but incomplete distinction between EC and EO, and in the filtered data, the same pattern, as well as pattern $\{2, 0, 1\}$ allows a complete distinction between the states.

An important advantage that our approach offers is the possibility of obtaining a good differentiation from the analysis of short time series. Distinguishing brain states from the analysis of EEG signals is an important open problem in neuroscience [31,34–36] that is particularly challenging when the analysis is performed real-time, i.e., while the data is being collected.

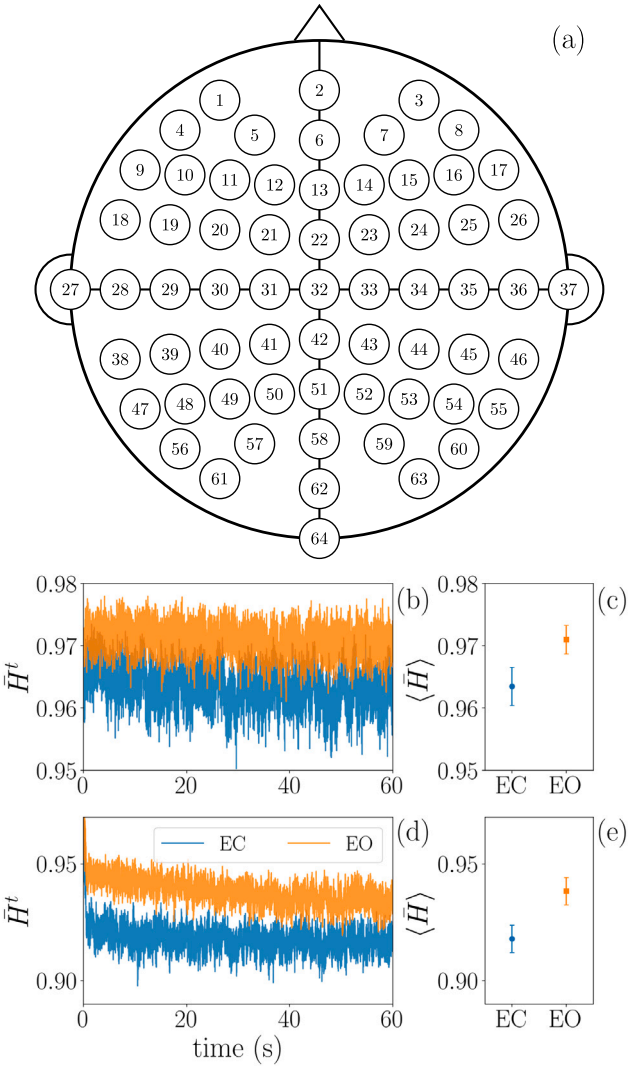

Fig. 6. New spatial arrangement. **(a)** A different spatial arrangement of the electrodes. The permutation entropy is calculated as in Fig. 5, but the electrodes are ordered in an alternative arrangement before calculating the ordinal patterns. **((b), (d))** Average over subjects of each state $\bar{H}^t$ for each time instant (Eq. (3)); **((c), (e))** Mean values over all time instants $\langle \bar{H} \rangle$ (Eq. (4)). This analysis shows a different arrangement that slightly improves the separation between states.

To show how our approach can be used in this situation, we analyze the EEG data considering time intervals whose duration is varied from 1 s to 60 s (whole data). Fig. 9 shows the temporal average of the spatial permutation entropy as a function of the duration of the time interval analyzed. Here, following the same approach as before, we analyze the EEG time series in a raw format (a) and also when an alpha filter is applied (b). The filtering is applied to the entire time series 60 s before the use of ordinal analysis. We observe that, in the raw data, our approach allows us to perfectly differentiate the two states by analyzing very short time intervals (20 s), and this time interval can be smaller in filtered data (3 s). We notice that in panel (a) the distinction between states is maximized in the first seconds. This can mistakenly lead us to think that the raw data analysis with small time intervals is more efficient for the distinction. We would like to emphasize that this is just a coincidence for that specific window of analysis. If we perform the same analysis of this figure but now not considering the first 10 s

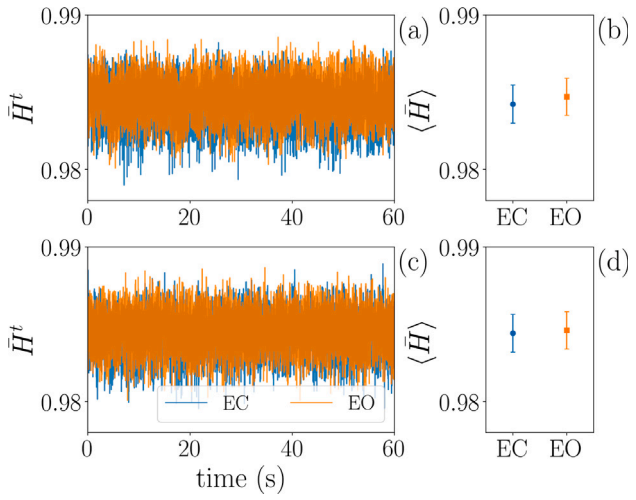

Fig. 7. Analysis of shuffled electrodes. The permutation entropy is calculated as in Fig. 5, but the electrodes are randomly shuffled before calculating the ordinal patterns. Shuffling the electrodes removes the spatial correlations and makes the two states indistinguishable.

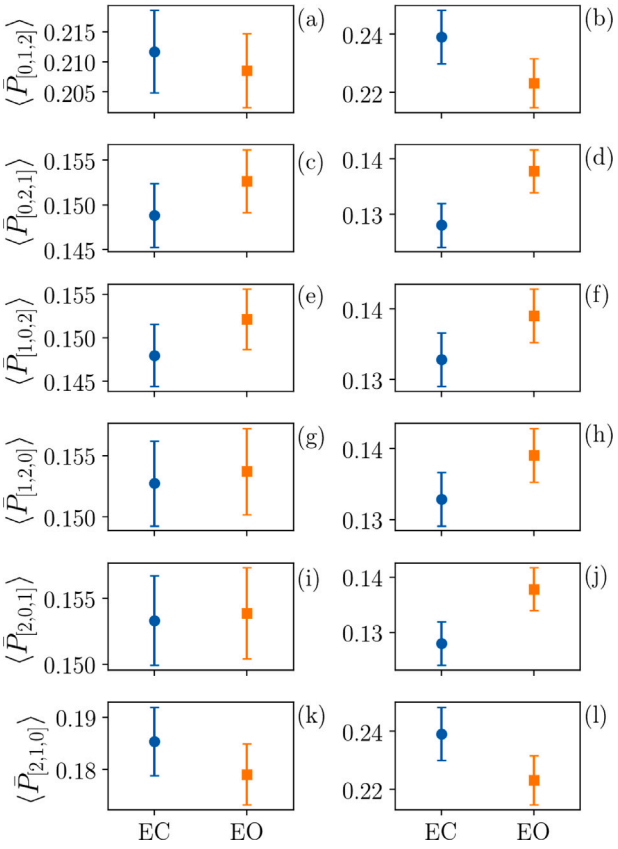

Fig. 8. Analysis of the ordinal probabilities. The 6 panels display the values of the 6 probabilities, averaged over time, and the bars display one standard deviation. Left panels present the results of the raw data and the right panels the filtered data. Here, we observe that some patterns give the opportunity to distinguish the resting brain states, just by calculating the pattern's probability.

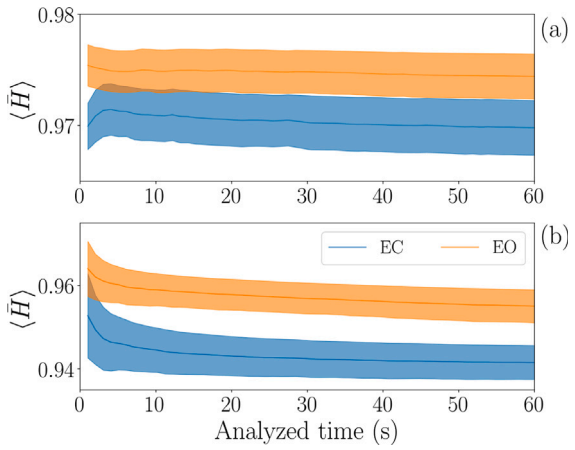

Fig. 9. Analysis of short time series. We calculate the averages over time intervals whose duration varies from 1 s to 60 s (whole time series), for the raw data **(a)**, and for the filtered data **(b)**. We see that in the raw data we can distinguish between the two resting states even when the time interval analyzed is very short.

of data, the difference between the two states is not maximum. We can conclude that with fewer data we do not necessarily have better results.

4. Conclusion

We have analyzed EEG data of healthy subjects that were asked to keep their eyes closed for one minute and then open their eyes. We have shown that the spatial permutation entropy, computed from spatial ordinal patterns (calculated at each time considering the spatial order of the data values in the electrodes), distinguishes the two brain states, a distinction that was not obtained when "temporal" ordinal analysis was used [22] (i.e., when the patterns were calculated by considering the temporal ordering of the data values). Our results, therefore, show that the spatial locations of the electrodes carries usable information. This was confirmed by shuffling the electrodes, which washed out spatial correlations and made the distinction impossible (Fig. 7).

The results obtained here improve the previous analysis [22] because here there is no overlap between bars, i.e. the two groups (EC and EO) can be separated, a fact that is even more pronounced in the filtered data (Fig. 5). The study of different configurations to find the optimal spatial arrangement is important for future research, as it could lead to a significant increase in the separation between the two states. Moreover, our results were obtained by analyzing the probabilities of patterns of length $D = 3$, while in [22], ordinal patterns of length $D = 4$ were used, which provides an additional advantage in terms of computational time (because only 6 probabilities, instead of 24, need to be calculated).

Importantly, we have shown that, in the raw data, the analysis of just a few seconds is sufficient to distinguish the brain states (Fig. 9), which opens the opportunity to use this methodology in "real-time" applications, such as brain-computer interface applications.

The differences detected are insufficient to distinguish the states at the individual-subject level. Future work will be devoted to combining temporal and spatial ordinal analysis with different embedding delays or spatial electrode arrangements to try to distinguish the states of individual subjects. In addition, the methodology used here can be useful to track more challenging problems, such as the classification of sleep/consciousness stages, the identification of intention of motion, etc.

Declaration of competing interest

The authors declare that they have no known competing financial interests or personal relationships that could have appeared to influence the work reported in this paper.

Data availability

Data is freely available in physionet.

Acknowledgments

B.R.R.B. and E.E.N.M. acknowledge support of São Paulo Research Foundation (FAPESP), Brazil, Proc. 2018/03211-6 and 2021/09839-0; and Financiadora de Estudos e Projetos (FINEP), Brazil. R.C.B. acknowledges support of Western Institute for Neuroscience Clinical Research Postdoctoral Fellowship and Western Academy for Advanced Research. K.L.R. acknowledges supported of German Academic Exchange Service (DAAD). C.M. acknowledges support of Ministerio de Ciencia, Innovación *y* Universidades (PID2021-123994NB-C21), Spain and Institució Catalana de Recerca i Estudis Avançats (ICREA), Spain.

References

[1] Bandt C, Pompe B. Permutation entropy: a natural complexity measure for time series. Phys Rev Lett 2002;88(17):174102.
[2] Bandt C. Small order patterns in big time series: A practical guide. Entropy 2019;21(6):613.
[3] Leyva I, Martinez JM, Masoller C, Rosso OA, Zanin M. 20 Years of ordinal patterns: Perspectives and challenges. Europhys Lett 2022;138:31001.
[4] Rosso OA, Larrondo HA, Martin MT, Plastino A, Fuentes MA. Distinguishing noise from chaos. Phys Rev Lett 2007;99(15):154102.
[5] Rosso OA, De Micco L, Larrondo HA, Martín MT, Plastino A. Generalized statistical complexity measure. Int J Bifurcation Chaos 2010;20(03):775–85.
[6] Zunino L, Soriano MC, Fischer I, Rosso OA, Mirasso CR. Permutation-information-theory approach to unveil delay dynamics from time-series analysis. Phys Rev E 2010;82(4):046212.
[7] Soriano MC, Zunino L, Rosso OA, Fischer I, Mirasso CR. Time scales of a chaotic semiconductor laser with optical feedback under the lens of a permutation information analysis. IEEE J Quantum Electron 2011;47(2):252–61.
[8] Aragoneses A, Carpi L, Tarasov N, Churkin DV, Torrent MC, Masoller C, et al. Unveiling temporal correlations characteristic to phase transition in the intensity of fibre laser radiation. Phys Rev Lett 2016;116:033902.
[9] Rosso OA, Masoller C. Detecting and quantifying stochastic and coherence resonances via information-theory complexity measurements. Phys Rev E 2009;79(4):040106.
[10] Boaretto BRR, Budzinski RC, Rossi KL, Prado TL, Lopes SR, Masoller C. Discriminating chaotic and stochastic time series using permutation entropy and artificial neural networks. Sci Rep 2021;11(1):1–10.
[11] Boaretto BRR, Budzinski RC, Rossi KL, Prado TL, Lopes SR, Masoller C. Evaluating temporal correlations in time series using permutation entropy, ordinal probabilities and machine learning. Entropy 2021;23(8):1025.
[12] Echegoyen I, Vera-Avila V, Sevilla-Escoboza R, Martinez JH, Buldu JM. Ordinal synchronization: Using ordinal patterns to capture interdependencies between time series. Chaos Solitons Fractals 2019;119:8–18.
[13] Acharya UR, Hagiwara Y, Koh JEW, Oh SL, Tan JH, Adam M, et al. Entropies for automated detection of coronary artery disease using ECG signals: A review. Biocybern Biomed Eng 2018;38(2):373–84.
[14] Faber J, Bozovic D. Chaotic dynamics of inner ear hair cells. Sci Rep 2018;8(1):1–9.
[15] Schlemmer A, Berg S, et al. Spatiotemporal permutation entropy as a measure for complexity of cardiac Arrhythmia. Front Phys 2018;6:39.
[16] Kottlarz I, Berg S, Toscano-Tejeida D, Steinmann I, Bähr M, Luther S, et al. Extracting robust biomarkers from multichannel EEG time series using nonlinear dimensionality reduction applied to ordinal pattern statistics and spectral quantities. Front Physiol 2021;11:614565.
[17] de Araujo FHA, Bejan L, Stosic B, Stosic T. An analysis of Brazilian agricultural commodities using permutation - information theory quantifiers: The influence of food crisis. Chaos Solitons Fractals 2020;139:110081.
[18] Tiana-Alsina J, Torrent MC, Rosso OA, Masoller C, Garcia-Ojalvo J. Quantifying the statistical complexity of low-frequency fluctuations in semiconductor lasers with optical feedback. Phys Rev A 2010;82(1):013819.
[19] Barreiro M, Marti AC, Masoller C. Inferring long memory processes in the climate network via ordinal pattern analysis. Chaos 2011;21(1):013101.
[20] Tirabassi G, Masoller C. Unravelling the community structure of the climate system by using lags and symbolic time-series analysis. Sci Rep 2016;6(1):1–10.
[21] Silva ASA, Menezes RSC, Rosso OA, Stosic B, Stosic T. Complexity entropy-analysis of monthly rainfall time series in northeastern Brazil. Chaos Solitons Fractals 2021;143:110623.
[22] Quintero-Quiroz C, Montesano L, Pons AJ, Torrent MC, García-Ojalvo J, Masoller C. Differentiating resting brain states using ordinal symbolic analysis. Chaos 2018;28(10):106307.
[23] Acharya UR, Hagiwara Y, Deshpande SN, Suren S, Koh JEW, Oh SL, et al. Characterization of focal EEG signals: a review. Future Gener Comput Syst 2019;91:290–9.
[24] Budzinski RC, Lopes SR, Masoller C. Symbolic analysis of bursting dynamical regimes of Rulkov neural networks. Neurocomputing 2021;441:44–51.
[25] Mateos DM, Gomez-Ramirez J, Rosso OA. Using time causal quantifiers to characterize sleep stages. Chaos Solitons Fractals 2021;146:110798.
[26] Abiri R, Borhani S, Sellers EW, Jiang Y, Zhao X. A comprehensive review of EEG-based brain–computer interface paradigms. J Neural Eng 2019;16(1):011001.
[27] Buzsaki G. Rhythms of the Brain. Oxford University Press; 2006.
[28] Buzsáki G, Wang X. Mechanisms of gamma oscillations. Annu Rev Neurosci 2012;35:203.
[29] Berger H. Über das elektroenkephalogramm des menschen. Arch Psychiatr Nervenkrankheiten 1929;87(1):527–70.
[30] Barry RJ, Clarke AR, Johnstone SJ, Magee CA, Rushby JA. EEG differences between eyes-closed and eyes-open resting conditions. Clin Neurophysiol 2007;118(12):2765–73.
[31] Petro NM, Ott LR, Penhale SH, Rempe MP, Embury CM, Picci G, et al. Eyes-closed versus eyes-open differences in spontaneous neural dynamics during development. NeuroImage 2022;258:119337.
[32] Thuraisingham RA, Tran Y, Boord P, Craig A. Analysis of eyes open, eye closed EEG signals using second-order difference plot. Med Biol Eng Comput 2007;45(12):1243–9.
[33] Gopan KG, Sinha N, Babu JD. Statistical feature analysis for EEG baseline classification: Eyes open vs eyes closed. In: 2016 IEEE Region 10 Conference. 2016, p. 2466–9. http://dx.doi.org/10.1109/TENCON.2016.7848476.
[34] Khosla A, Khandnor P, Chand T. A novel method for EEG based automated eyes state classification using recurrence plots and machine learning approach. Concurr Comput: Pract Exper 2022;e6912.
[35] Furman Ł, Duch W, Minati L, Tołpa K. Short-time Fourier transform and embedding method for recurrence quantification analysis of EEG time series. Eur Phys J Spec Top 2022;1–15.
[36] Lai CQ, Ibrahim H, Suandi SA, Abdullah MZ. Convolutional neural network for closed-set identification from resting state electroencephalography. Mathematics 2022;10(19):3442.
[37] Muller L, Chavane F, Reynolds J, Sejnowski TJ. Cortical travelling waves: mechanisms and computational principles. Nat Rev Neurosci 2018;19(5):255–68.
[38] Muller L, Piantoni G, Koller D, Cash SS, Halgren E, Sejnowski TJ. Rotating waves during human sleep spindles organize global patterns of activity that repeat precisely through the night. Elife 2016;5:e17267.
[39] Davis ZW, Muller L, Martinez-Trujillo J, Sejnowski T, Reynolds J. Spontaneous travelling cortical waves gate perception in behaving primates. Nature 2020;587(7834):432–6.
[40] Ribeiro HV, Zunino L, Lenzi EK, Santoro PA, Mendes RS. Complexity-entropy causality plane as a complexity measure for two-dimensional patterns. PLoS One 2012;7:e40689.
[41] Sigaki HYD, de Souza RF, de Souza RT, Zola RS, Ribeiro HV. Estimating physical properties from liquid crystal textures via machine learning and complexity-entropy methods. Phys Rev E 2019;99:013311.
[42] Tirabassi G, Masoller C. Entropy-based early detection of critical transitions in spatial vegetation fields. Proc Natl Acad Sci USA 2023;120:e2215667120.
[43] Repository with the EEG Dataset: https://physionet.org/content/eegmmidb/1.0.0/ We have discarded subjects #97 and #109 due to several null values at the end of the time series.
[44] Schalk G, McFarland DJ, Hinterberger T, Birbaumer N, Wolpaw JR. BCI2000: a general-purpose brain-computer interface (BCI) system. IEEE Trans Biomed Eng 2004;51(6):1034–43.
[45] Goldberger AL, Amaral LAN, Glass L, Hausdorff JM, Ivanov PC, Mark RG, et al. PhysioBank, PhysioToolkit, and PhysioNet: components of a new research resource for complex physiologic signals. Circulation 2000;101(23):e215–20.
[46] Virtanen P, Gommers R, Oliphant TE, Haberland M, Reddy T, Cournapeau D, et al. SciPy 1.0: Fundamental algorithms for scientific computing in python. Nature Methods 2020;17:261–72. http://dx.doi.org/10.1038/s41592-019-0686-2.